Pergamon

Journal of Structural Geology, Vol. 18, Nos 2/3, pp. 169 to 178, 1996

0191-8141/96 $15.00 + 0.00

0191-8141(95)00101-8

Aggregate properties of fracture populations

RANDALL MARRETT

Department of Geological Sciences, University of Texas at Austin, Austin, TX 78712, U.S.A.

(*Received* 23 *January* 1995; *accepted in revised form* 17 *August* 1995)

Abstract—Empirical studies indicate that the individual attributes of both faults and extension fractures follow power-law scaling. Aggregate properties of fracture populations are important in a variety of problems and can be specified in terms of the scaling parameters of individual fracture attributes. Development of an expression for an aggregate property requires consideration of a number of independent factors, including the topologic dimension of the aggregate property, the topologic dimension of sampling and the possibility of scaling changes for fractures that span some mechanically significant layer. The Riemann zeta function provides an alternative to integration for the analytical and numerical solution of aggregate problems.

Previous work regarding aggregate properties of fracture populations has focused on the strain due to faulting. New expressions are developed here for other aggregate properties of interest: fracture surface area, fracture porosity, fracture permeability and shear-wave anisotropy. A general characteristic of these aggregate properties is that, for most values of scaling exponents, the aggregate properties are dependent on the size of the sampling domain. This implies that the aggregate properties are scale-dependent. Additionally, it appears that fracture surface area is concentrated in the smallest fractures of many populations. Fracture porosity is concentrated in the largest fractures of most populations but not as strongly as fracture permeability, which probably derives almost entirely from the largest fractures in populations.

INTRODUCTION

Many empirical studies have demonstrated that a variety of shear and extension fracture attributes commonly exhibit power-law scaling (e.g. Kakimi 1980, Shaw & Gartner 1986, Gudmundsson 1987a, Villemin & Sunwoo 1987, Childs *et al.* 1990, Heffer & Bevan 1990, Scholz & Cowie 1990, Walsh *et al.* 1991, Jackson & Sanderson 1992, Marrett & Allmendinger 1992, Davy 1993, Peacock & Sanderson 1994, Wojtal 1994, Carter & Winter 1995). Knowledge of these scaling relations is sufficient to address some problems directly, such as the relative abundance of fractures in different size ranges; however, many problems center on the aggregate properties of a fracture population rather than the attributes of individual fractures. For example, strain due to faulting, fluid permeability of rock containing open fractures and shear-wave anisotropy due to fractures are most meaningful in reference to entire fracture populations. Such aggregate properties may be expressed in terms of individual fracture attributes and generalized with the scaling relations of those attributes; however, a number of fundamental issues must be addressed first.

Aggregate properties of fracture populations may be expressed in some cases as linear, surficial or volumetric parameters. The individual fracture attributes used to express the aggregate properties depend on the aggregate definition chosen. An additional complication stems from the limitation that fracture observations usually are limited to one- or two-dimensional samples, so the topologic dimension of sampling commonly differs from that of the desired aggregate property. This requires an understanding of how fracture-attribute scaling varies with the topologic dimension of sampling. One also must consider the possibilities of scaling changes at mechanical boundaries of a fracture population, such as imposed by sedimentary layering or the finite thickness of the schizosphere. Scaling changes might simply reflect the topologic difference between the regions occupied by fractures at different scales, but the changes could be more fundamental. Finally, a variety of mathematical techniques are available to express aggregate properties in terms of the scaling of individual fracture attributes. The Riemann zeta function has not been used previously in this context, but it should provide better accuracy than integral expressions of aggregate properties.

The objectives of this contribution are (1) to review the scaling of some key fracture attributes and develop all relationships among the scaling parameters; (2) to examine in detail the issues mentioned above, which are the source of significant confusion and are general problems in estimating aggregate properties; and (3) to derive specific expressions for a variety of important aggregate properties of fracture populations. Hopefully, the aggregate expressions developed here will be useful not only for the problems considered, but also as illustrations for the formulation of other aggregate properties.

FRACTURE SCALING RELATIONS

The scaling of fault populations has received much attention during the past decade. Consensus indicates that the cumulative number of faults (N) in a specific

Table 1. Notation

Term	Meaning
N	Cumulative number of faults or extension fractures
R	Size of sampling domain (length, area or volume)
D	Fault displacement
L	Fault length
δ	Fault heave
M_g	Fault geometric moment
b	Extension fracture aperture
l	Extension fracture length
λ	Fracture plane ellipticity
A	Coefficient of N–D power law for faults
C	Exponent of N–D power law for faults
H	Coefficient of N–L power law for faults
E	Exponent of N–L power law for faults
G	Coefficient of D–L power law for faults
M	Exponent of D–L power law for faults
a	Coefficient of N–b power law for extension fractures
c	Exponent of N–b power law for extension fractures
h	Coefficient of N–l power law for extension fractures
e	Exponent of N–l power law for extension fractures
g	Coefficient of b–l power law for extension fractures
m	Exponent of b–l power law for extension fractures
B	Exponent of N–M_g power law for faults
ζ	Riemann zeta function
ε	Fault strain
σ	Fracture surface area
ϕ	Extension fracture porosity
k	Extension fracture permeability
γ	Shear-wave anisotropy
v	Shear-wave velocity

region having displacement $\geq D$ or length $\geq L$ may be expressed as:

$$N = RAD^{-C} \tag{1a}$$

or

$$N = RHL^{-E}, \tag{1b}$$

where R is the size of the sampling domain and A, H, C and E are empirical scaling constants (see Table 1 for summary of notation; Kakimi 1980, Shaw & Gartner 1986, Gudmundsson 1987a, Villemin & Sunwoo 1987, Childs *et al.* 1990, Heffer & Bevan 1990, Scholz & Cowie 1990, Walsh *et al.* 1991, Jackson & Sanderson 1992, Marrett & Allmendinger 1992, Walsh & Watterson 1992, Davy 1993, Scholz *et al.* 1993, Marrett 1994, Patton *et al.* 1994, Peacock & Sanderson 1994, Wojtal 1994, Carter & Winter 1995, Gross & Engelder 1995, Cladouhos & Marrett 1996). In a statistical sense, displacement and length scale as:

$$D = GL^{M}, \tag{1c}$$

where G and M are empirical scaling constants (Walsh & Watterson 1988, Scholz & Cowie 1990, Marrett & Allmendinger 1991, Cowie & Scholz 1992, Gillespie *et al.* 1992, Dawers *et al.* 1993). Thus, the exponents of the power laws are related by $E = MC$ and the coefficients by $A = G^{C}H$, from which we see there are only four independent scaling constants for the length and displacement attributes of a fault population. Additionally, by setting $N = 1$, we find that $A = D_1^{C}/R$ and $H = L_1^{E}/R$, where subscripts of fault attributes refer to the value of N.

More recent work has led to the development of similar relations for populations of extension fractures. The cumulative number of extension fractures (N) in a specific region having aperture (and/or mineral-fill thickness) $\geq b$ or length $\geq l$ may be expressed as:

$$N = Rab^{-c} \tag{2a}$$

or

$$N = Rhl^{-e}, \tag{2b}$$

where R is the size of the sampling domain and a, h, c and e are empirical scaling constants (Gudmundsson 1987b, Barton & Hsieh 1989, Wong *et al.* 1989, Heffer & Bevan 1990, Barton & Zoback 1992, Hatton *et al.* 1993, McCaffrey *et al.* 1993, 1994, Sanderson *et al.* 1994, Gross & Engelder 1995). Aperture and length scale as:

$$b = gl^{m}, \tag{2c}$$

where g and m are empirical scaling constants (Johnston 1992, 1994, Hatton *et al.* 1994, Vermilye & Scholz 1995). Thus, the exponents of the power laws are related by $e = mc$ and the coefficients by $a = g^{c}h$, from which we see there are only four independent scaling constants for the length and aperture attributes of an extension fracture population. Additionally, by setting $N = 1$ we find that $a = b_1^{c}/R$ and $h = l_1^{e}/R$, where subscripts of fracture attributes refer to the value of N.

THEORETICAL CONSIDERATIONS

The notion of 'dimension' may enter into problems of aggregate properties of fracture populations in at least five forms, generating both semantic and conceptual confusion. (1) The aggregate property may be tensorial; (2) the aggregate property may describe spatial regions of different dimension; (3) the sampling of individual fractures in a population may be done along a line, over a surface or through a volume; (4) the scaling of individual fracture attributes may be considered fractal in some contexts, introducing the concept of fractal dimension; and (5) the attribute scaling of fractures that have reached critical dimensions defined by the fractured region may differ from the attribute scaling of fractures that have not reached such critical dimensions. Each of these aspects of an aggregate problem are distinct.

The tensorial character of some aggregate properties is dimensional in the sense, for example, that strain may be considered simultaneously in all spatial directions about a point (three-dimensional strain ellipsoid) or in only one particular direction (one-dimensional longitudinal strain). This is clearly distinct from the other dimensions. The second and third aspects are akin to one another, but distinct. An aggregate property may refer to phenomena along a line, over a surface or though a volume; sampling may describe phenomena in the same topologies. However, the dimensions of an aggregate property and sampling can differ, for example when attempting to address the strain through a three-dimensional volume based on data collected along a line or a surface passing through the volume. Ideally, the aggregate property and sampling dimensions would

Table 2. Relationships among power-law exponents and coefficients for different sampling topologies

	Exponents			Coefficients
Small faults	$C_V=C_S+1/M=C_T+2/M$	$E_V=E_S+1=E_T+2$	$A_VC_V=\lambda A_SC_SG^{1/M}=4\lambda A_TC_TG^{2/M}/\pi$	$H_VE_V=\lambda H_SE_S=4\lambda H_TE_T/\pi$
Small extension fractures	$c_V=c_S+1/m=c_T+2/m$	$e_V=e_S+1=e_T+2$	$a_Vc_V=\lambda a_Sc_Sg^{1/m}=4\lambda a_Tc_Tg^{2/m}/\pi$	$h_Ve_V=\lambda h_Se_S=4\lambda h_Te_T/\pi$
Large faults	$C_V=C_S=C_T+1/M$	$E_V=E_S=E_T+1$	$A_VC_V=A_SC_S=A_TC_TG^{1/M}$	$H_VE_V=H_SE_S=H_TE_T$
Large extension fractures	$c_V=c_S=c_T+1/m$	$e_V=e_S=e_T+1$	$a_Vc_V=a_Sc_S=a_Tc_Tg^{1/m}$	$h_Ve_V=h_Se_S=h_Te_T$

Subscripts of scaling constants indicate sampling topology: *V—volumetric sampling*, *S—surficial sampling* (on planes perpendicular to minor axes of elliptical fractures) and *T—linear sampling* (on lines perpendicular to fractures); λ is ellipticity of small fractures, as defined by ratio of major axis to minor axis lengths.

always be equal, but they commonly differ due to sampling limitations. Both are considered in detail below, where they are referred to as the topologic dimensions of a problem. The aspect of fractal dimensions is not explicitly germane to the discussion in this paper, which is independent of the specific *spatial* distribution of fractures, so the concept is not further pursued. However, the observed scaling parameters of fracture attribute *size* distributions usually depend on the sampling topology and these relationships are fully developed below. The fifth aspect is often confused with the second and third, with which it may be related despite being fundamentally independent. The systematics of scaling changes within a population that spans the critical dimension of a fractured region are not yet understood, but some possibilities are outlined below. The final theoretical topic addressed in this section is the analytic and numerical evaluation of aggregate properties from individual fracture attribute scaling. Integration, summation and use of the Riemann zeta function are each considered.

Topologies of aggregate property and sampling

The topology of a problem of aggregate properties is significant in two ways. First, the aggregate property to be analyzed has an implicit or explicit topologic dimension. In some cases, one may choose the topologic dimension of the aggregate property to suit the available data (see following paragraph) or the problem at hand. For example, we may address fault strain along a line, over a surface or through a volume. The choice is nontrivial, because the appropriate expression for fault strain varies according to our choice. For scalar representation of strain within a volume, the strain resulting from the displacement on a fault is the geometric moment of the fault (average displacement times fault area) divided by the volume of the region of interest (e.g. Marrett & Allmendinger 1990). In this case, we may think of the fault-area term of the geometric moment as a weighting term. For strain over a surface, the two-dimensional analog to the geometric moment is the product of average fault displacement (averaged along the intersection of the fault with the surface of interest) and fault length, so the displacements of faults in a population are weighted by the fault lengths. For longitudinal strain along a line (referred to below as linear strain), the one-dimensional analog to the geometric moment is simply the fault displacement where the line of interest crosses the fault. The faults in a population are not weighted differentially because each fault occupies an identical portion of the line (i.e. a point). Consequently, a linear strain estimate may be determined independently of the fault length distribution and the fault displacement–length relation, so fault lengths do not enter into the problem (Marrett & Allmendinger 1992). Nevertheless, as demonstrated by Peacock & Sanderson (1993), fault strain analysis along a line or over a surface is not limited to zeroth- or first-order tensors. The important point is that the topologic dimension of the aggregate property of interest may determine the individual fracture attributes needed to solve a problem.

The second way topology enters a problem of aggregate properties is via sampling. Although some of the aggregate properties we may wish to determine for a population of fractures are three-dimensional, most data sets represent one-dimensional (scanline or borehole) or two-dimensional (map or cross-section) sampling of fracture populations. In some cases, it is possible to express an aggregate problem to accommodate the topologic dimension with which sampling is most confidently done. However, in many cases, one needs to compare independent data sets collected with different topologies (e.g. Marrett 1994) or the aggregate property of interest is only meaningful at a topologic dimension infeasible for sampling (e.g. see section entitled *Extension fracture shear-wave anisotropy* below). This requires an understanding of how sampling topology affects observed fracture-attribute scaling.

Theoretical arguments and numerical experiments suggest that observed scaling parameters vary with sampling topology in a systematic manner. If fracture locations and aspect ratios of fracture surfaces are uncorrelated with fracture sizes and orientations and if the fractures are embedded in a three-dimensional volume (i.e. 'small' fractures, see following section), then the probability of sampling a specific fracture is then proportional to the fracture area (i.e. length squared) for one-dimensional samples and proportional to the fracture length for two-dimensional samples (Marrett & Allmendinger 1991). Specific relationships among the exponents and coefficients for the different sampling topologies (Table 2) follow immediately from the sam-

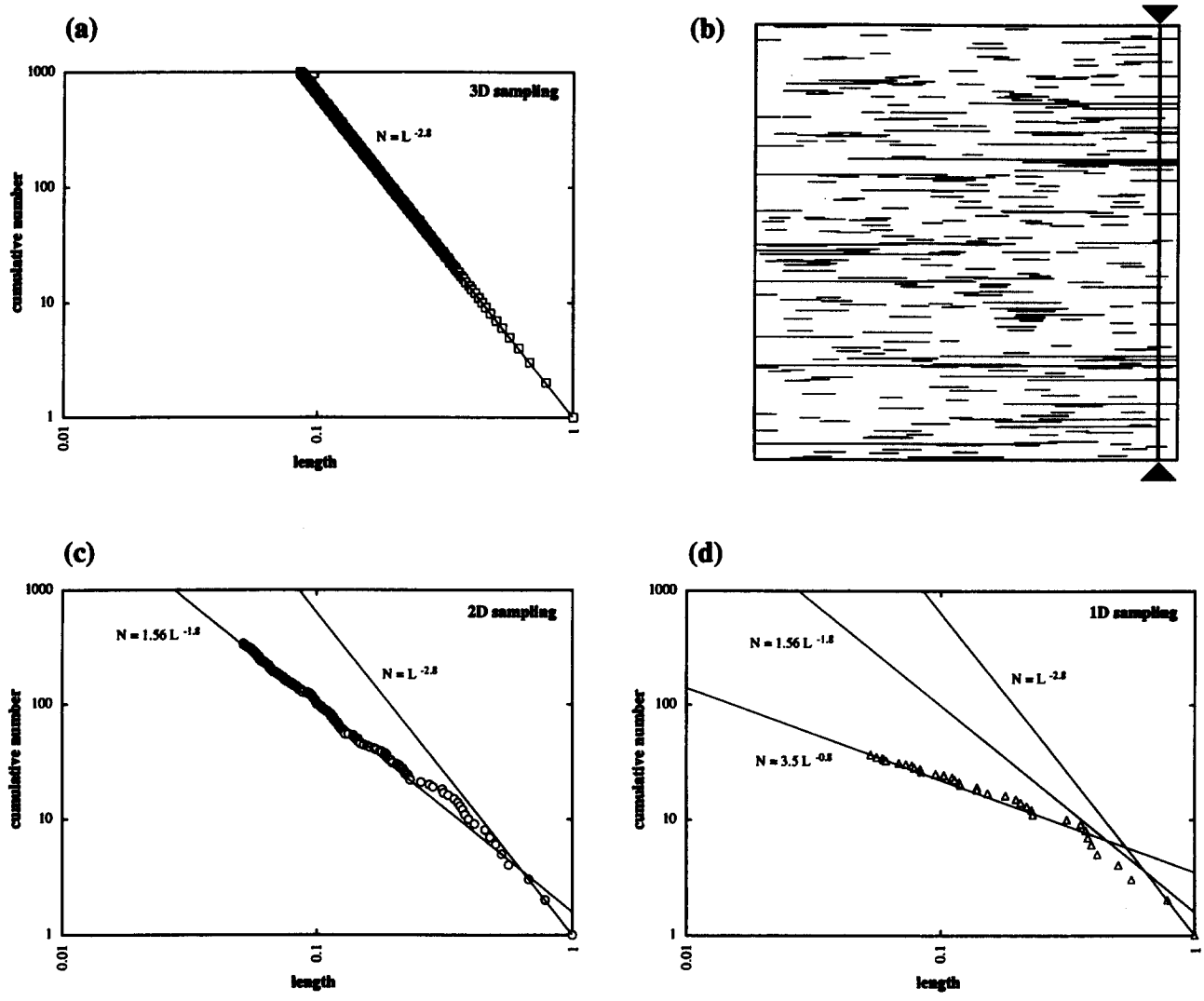

Fig. 1. Numerical experiment illustrating effect of sampling topology. (a) Cumulative number–length plot for fractures in three-dimensional (complete) sample, following $N = L^{-2.8}$. (b) Map view of 334 fractures in a two-dimensional sample from a synthetic three-dimensional population comprising 4000 fractures, with bold line showing position of one-dimensional sample (36 fractures). (c) Cumulative number–length plot for fractures in two-dimensional sample, which follow theoretical prediction of $N=1.56l^{-1.8}$. (d) Cumulative number–length plot for fractures in one-dimensional sample, which follow theoretical prediction of $N=3.5l^{-0.8}$. The lines shown in (c) and (d) are not empirical regressions to the data, but instead were determined analytically using the relations given in Table 2.

pling topologies and discrete numbers (the derivatives of cumulative numbers) by assuming that one- and two-dimensional samples are taken perpendicular to the fracture orientations and that the fractures have elliptical surfaces (Marrett & Allmendinger 1991, Westaway 1994).

The relations among scaling parameters for fractures that span a two-dimensional shell (i.e. 'large' fractures, see following section) are slightly different. In this case a shell-parallel two-dimensional sample reveals the entire three-dimensional population (probability of sampling equals 1 for all large fractures), and the probability of sampling a specific fracture in a shell-parallel one-dimensional sample (or a shell-perpendicular two-dimensional sample) is proportional to the fracture length (Marrett & Allmendinger 1991). The relationships among exponents and coefficients for shell-parallel samples (Table 2) follow from the assumption that one- and two-dimensional samples are taken perpendicular to the fracture orientations and that the fractures have rectangular surfaces.

A numerical experiment illustrates the sample-topology effect with a synthetic three-dimensional population of 4000 square fractures generated such that E_V = 2.8 and H_V = 1 (Fig. 1a). The fractures were located randomly within a cube having edges equal in length to the largest fracture, and the fractures parallel one side of the cube. Two- and one-dimensional samples were taken perpendicular to the fractures at random positions through the volume (Fig. 1b). The lengths of fractures in the two-dimensional sample (Fig. 1c) are consistent with the values of E_S = 1.8 and H_S = 1.56 predicted theoretically (Table 2) and the lengths of fractures in the one-dimensional sample (Fig. 1d) are consistent with the values of E_T = 0.8 and H_T = 3.5 predicted theoretically (Table 2). Notice that the steep segments of the length–

number plots for the longest fractures in the one- and two-dimensional samples are not sampling artifacts, but a systematic result of low-topology sampling. These steep segments are not the result of censoring (e.g. Baecher & Lanney 1978, Barton & Zoback 1992); they may reinforce censoring artifacts in natural fracture populations and might be confused with censoring artifacts.

Changes in scaling

Although the fracture scaling relations are conventionally written in a form that ignores limits, it is clear that limits must exist. We expect fracture scaling to have a lower limit imposed by changes in material properties and boundary conditions at the scale of mineral grains (Walsh & Watterson 1992). An upper limit for faults is imposed by the finite thickness of the schizosphere. For example, earthquakes that span the schizosphere ('large' earthquakes) scale, but they do so in a manner distinct from earthquakes contained by the schizosphere ('small' earthquakes) and the details of the change are as yet controversial (e.g. Main 1992, Pacheco *et al.* 1992, Romanowicz & Rundle 1993, Scholz 1994).

Based on the change in earthquake scaling, it is reasonable to conjecture that the scaling of large faults differs from that of small faults; however, too few data are available to reach conclusions. Additionally, due to the limitations of fault sampling, it is difficult to adequately compare the scaling of large and small faults. Some low-topology data sets (e.g. one-dimensionally sampled displacements of Walsh *et al.* 1991) appear to show consistent power-law exponents across the large/small transition ($C_{T_{large}} = C_{T_{small}}$), indicating a change in scaling for the complete three-dimensional fault population ($C_{V_{large}} = C_{T_{large}} + 1/M$, but $C_{V_{small}} = C_{T_{small}} + 2/M$). However, other low-topology data sets (e.g. two-dimensionally sampled lengths of Marrett 1994) appear to show more negative exponents for large faults than for small faults ($E_{S_{large}} = 1 + E_{S_{small}}$?), possibly indicating consistent scaling across the large/small transition for the complete three-dimensional fault population ($E_{V_{large}} = E_{S_{large}} = E_{V_{small}} = E_{S_{small}} + 1$). More data sets are needed in which large and small faults from a single region may be studied.

It is also possible that the upper limit of fracture scaling will occur at a significantly smaller scale than the thickness of the schizosphere. Fractures may be confined to specific litho-mechanical layers (e.g. Gross & Engelder 1995), such that fracture scaling in one layer is only indirectly related to scaling in other layers. Even where some fractures span a significant litho-mechanical layer, the layer thickness may define distinct populations of intra- and trans-layer fractures. A special case of this idea is the hypothesis that intra-horse faults (i.e. those bounded by tip lines) and horse-bounding faults (i.e. those bounded by branch lines) in a duplex system scale differently (Wojtal 1994). Subsequent usage of the terms 'large' and 'small' in this paper will reflect this more general reference to any mechanically significant layer.

Evaluation

A final theoretical hurdle that must be overcome to estimate aggregate properties for a population of fractures is evaluation of the appropriate expression of individual fracture attributes. A common form of evaluation is integration (e.g. Scholz & Cowie 1990, Westaway 1994); however, this implicitly treats the discontinuous size distributions of fracture attributes as continuous functions. Integration generally results in an underestimate of aggregate properties (Marrett & Allmendinger 1991). For example, in equation (7) of Scholz & Cowie (1990) $C < 1.5$ implies that the total geometric moment of a fault population is less than the geometric moment of the single largest fault and $C = 0$ (i.e. only one fault) implies that the total geometric moment is zero. Clearly, it is preferable to use summation of actual data when estimating aggregate properties for a specific problem; integration may be satisfactory when accounting for fractures underrepresented in a data set (Marrett & Allmendinger 1992) due to truncation (e.g. Baecher & Lanney 1978, Barton & Zoback 1992).

For purposes of evaluating the sensitivity of aggregate properties to the relevant power-law exponent, it is also desirable to formulate closed-form analytical expressions for aggregate properties. Integration provides one method of deriving such expressions (e.g. Scholz & Cowie 1990); however, as indicated above, the results of integration can yield non-physical results. A more accurate alternative to integration is provided by the Riemann zeta function (Apostal 1957), which is implicit in a general expression of aggregate properties. The Riemann zeta function (ζ) is the infinite series:

$$\zeta(x) = 1 + 2^{-x} + 3^{-x} + 4^{-x} \ldots \quad (3)$$

and converges for arguments $x > 1$. Note that ζ may be substituted into equation (12) of Marrett & Allmendinger (1991):

$$M_{g_{total}} = M_{g_1}[1 + 2^{-1/B} + 3^{-1/B} + 4^{-1/B} \ldots], \quad (4)$$

yielding

$$M_{g_{total}} = \zeta\left(\frac{1}{B}\right) M_{g_1}, \quad (5)$$

where M_{g_1} is the geometric moment of the largest fault, $M_{g_{total}}$ is the total geometric moment of the fault population and B is the power-law exponent of the geometric moment size distribution. Equation (5) is an equally compact, but more accurate, alternative to the equivalent integral formulation [equation (13) of Marrett & Allmendinger 1991]:

$$M_{g_{total}} = \frac{B}{1 - B} M_{g_1}. \quad (6)$$

A good approximation to the Riemann zeta function (accurate to three significant figures) may be obtained by summing the first three terms of the infinite series and taking the first two terms of the Euler–Maclauren sum-

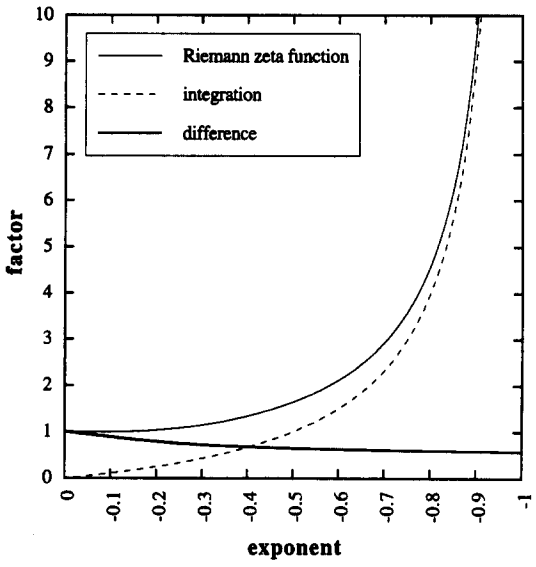

Fig. 2. Comparison of Riemann zeta function (thin curve) and integration (dashed curve) formulations of aggregate properties. Thick curve shows the difference between the factors for the two formulations. Exponent refers to any exponent of a fracture attribute (e.g. fault geometric moment, extension fracture aperture, etc.) in a power-law size distribution of the appropriate form for aggregate property evaluation, regardless of the sampling topology.

mation formula (Dahlquist & Björck 1974) to express the remainder:

$$\zeta(x) \cong 1 + 2^{-x} + 3^{-x} + \frac{x+7}{2(x-1)} 4^{-x}. \qquad (7)$$

The Euler–Maclauren summation formula may also be used as an alternative to integration when accounting for fractures under-represented in a data set due to truncation. For example, equation (4) of Marrett & Allmendinger (1992) becomes:

$$\delta_{\text{extrapolation}} \cong \delta_N \frac{C}{1-C}\left(N + \frac{1}{2} + \frac{1}{2C}\right)\left(\frac{N}{N+1}\right)^{1/C}, \qquad (8)$$

where δ_N is fault heave of the Nth largest fault and $\delta_{\text{extrapolation}}$ is the cumulative heave of faults over the size range affected by sampling truncation. As expected, the integral formulation for fractures affected by sampling truncation underestimates their contribution to the aggregate property, although the deficit greatly diminishes as N increases. In some natural examples (e.g. Peacock & Sanderson 1994) the exponent of the relevant power-law [e.g. $B \geq 1$ in equation (5)] leads to a non-convergent infinite series of the Riemann function. In most of these cases, an expression equivalent to equation (8) may be used to truncate the Riemann function and derive a finite result. The exception to this is the case where the power-law exponent exactly equals one, in which case the integral formulation of Westaway (1994) is the only solution known to the author.

Both the Riemann and integral formulations of an aggregate property [e.g. equations (5) and (6)] may be expressed as the product of the relevant term for the largest fracture and a factor that depends on the exponent of the appropriate scaling relation [e.g. equation (3) of Marrett & Allmendinger 1991]. Figure 2 shows how this factor for Riemann and integral formulations varies as a function of the exponent. The factor for integration is less than the factor for the Riemann zeta function over the entire range of possible exponents. Note that the factor for the Riemann formulation is always greater than one, except when the exponent is zero (i.e. only one fracture). Unlike the integral formulation, the Riemann formulation provides meaningful results for all convergent values of the power-law exponent.

AGGREGATE PROPERTIES

A variety of aggregate properties of fracture populations are important to many problems. Most previous work on aggregate properties has been limited to fault strain. Other important aggregate properties include total fracture surface area, extension fracture porosity, extension fracture permeability and extension fracture shear-wave anisotropy. Below, I present treatments for these aggregate properties from the scaling of individual fracture attributes.

Subscripts are required here in four ways. As above, the subscripts V, S and T indicate sampling topology when used with scaling parameters and sampling domain size. However, the same subscripts used with aggregate properties indicate aggregate property topology, which may differ from sampling domain topology. The subscripts *large* and *small* refer to large and small fractures relative to some mechanically significant layer. And the subscripts 1 and *min* modify individual fracture attributes to indicate the largest or smallest fracture in a population.

Fault strain

Aggregate strain estimates based on fault-attribute scaling have been developed in a variety of contexts (Marrett & Allmendinger 1990, 1992, Scholz & Cowie 1990, Walsh *et al.* 1991, Jackson & Sanderson 1992, Patton *et al.* 1994, Westaway 1994, Carter & Winter 1995, Gross & Engelder 1995). These analyses have taken a variety of forms representing different sampling or aggregate topologies. Westaway (1994) provided the most general analysis to date but did not analytically address both large and small faults nor the possible scaling change at that point, which might follow systematic patterns. Because a complete treatment simultaneously accounting for aggregate property topology, sampling topology, large and small faults and general scaling changes has not been developed previously, one is presented here.

As described above, strain is determined differently according to the topology of the region considered, which may be a line (R_T), a surface (R_S) or a volume (R_V). For incremental deformation (i.e. $D \ll R_T$), the longitudinal strain along a line sample ε_T (referred to below as linear strain) is simply the sum of appropriate displacement components D divided by the sampling

domain size R_T (e.g. Peacock & Sanderson 1993), yielding for small faults alone:

$$\varepsilon_T = \sum \frac{D_{small}}{R_T} = \zeta\left(\frac{1}{C_{T_{small}}}\right)\frac{D_1}{R_T}, \quad (9a)$$

from substitution of equations (1a) and (3) into the summation, or:

$$\varepsilon_T = \zeta\left(\frac{1}{C_{T_{small}}}\right)A_{T_{small}}^{(1/C_{T_{small}})}R_T^{(-1+(1/C_{T_{small}}))}, \quad (9b)$$

by setting $N = 1$ in equation (1a), solving for D_1 and substituting the result into equation (9a). The advantage of equation (9b) over (9a) is that strain is specified in terms of only the coefficient and exponent of the scaling law (neither of which will vary with sampling domain size) and the size of the sampling domain. An important result is that fault strain depends on sample size (except when the argument of the Riemann zeta function is equal to one), indicating that fault strain generally is scale dependent. For a combination of large and small faults:

$$\begin{aligned}\varepsilon_T &= \sum \frac{D_{large}}{R_T} + \sum \frac{D_{small}}{R_T} \\ &= \zeta\left(\frac{1}{C_{T_{large}}}\right)A_{T_{large}}^{(1/C_{T_{large}})}R_T^{(-1+(1/C_{T_{large}}))} \\ &\quad - \frac{D_x}{R_T}\left[\frac{C_{T_{large}}}{1-C_{T_{large}}}\left(A_{T_{large}}R_T D_x^{-C_{T_{large}}} - \frac{1}{2} + \frac{1}{2C_{T_{large}}}\right)\right] \\ &\quad + \frac{D_x}{R_T}\left[\frac{C_{T_{small}}}{1-C_{T_{small}}}\left(A_{T_{small}}R_T D_x^{-C_{T_{small}}} - \frac{1}{2} + \frac{1}{2C_{T_{small}}}\right)\right],\end{aligned} \quad (9c)$$

where D_x is the critical displacement needed for faults to become large, the scaling parameters for large and small faults are treated as independent and expressions equivalent to equation (8) are substituted (last two terms) to account for the change in scaling. A simpler expression will result once the relationships between large- and small-fault scaling parameters are understood. Linear strain may be calculated using displacement scaling parameters from non-linear sampling or using length scaling parameters by applying the various relations of Table 2. These equations for linear strain converge if $C_{T_{small}} < 1$, although $C_{T_{large}} > 1$ requires an alternative expression for the strain due to large faults in equation (9c). Expressions similar to equations (9) may be developed for longitudinal strain in a specific direction along a surface by summing the products of the appropriate displacement and length components for each fault and dividing by the area of the sampling domain. Likewise, the longitudinal strain in a volume is attained by summing the products of the appropriate displacement component and projected area for each fault and dividing by the volume of the sampling domain.

One alternative form of the linear strain due to small faults [equation (9a)] is the product of the Riemann zeta function and the strain due to the largest fault. Values determined for $C_{T_{small}}$ commonly fall between 0.7 and 0.9 (e.g. see references under section entitled *Fracture scaling relations* above), suggesting that the total fault strain for a population of small faults is typically 2.9–9.6 times the strain due to the single largest fault. However, the effect illustrated in Fig. 1 will cause the largest faults in a one-dimensional sample to have smaller displacements than predicted by the power law describing the rest of the population, assuming the entire population of small faults follows a power law in three dimensions. Consequently, the total fault strain will be greater than the estimate yielded by equation (9a), but less than the estimate yielded by equation (9b). These problems are eliminated in natural examples for which sufficient data are available by summing the strain due to the largest faults and using analytical expressions to account for the strain due to smaller faults. Equations (9) are provided as a conceptual guide to how the various parameters influence strain. Despite the complex form of equations (9) and their two- and three-dimensional equivalents, they involve at most four independent scaling parameters if large and small scaling parameters can be expressed in terms of each other.

Fracture surface area

Aggregate estimates of total fracture surface area based on fracture scaling relations apparently have not been developed previously, however total fracture surface area may be important in a variety of contexts. For example, many chemical processes are sensitive to the area of fluid/solid interface, and mechanical energy is consumed in fracture surface generation during faulting. Unlike strain, fracture surface area is only meaningful in volumetric terms. Aggregate fracture surface area also differs from the strain equivalent in that most observed scaling parameters suggest that the quantity does not converge (i.e. the argument of the Riemann zeta function is less than one). Nevertheless, the total fracture surface area (σ_V) may be determined by using the approximation for the Riemann zeta function [equation (7)] and truncating the sum at the lower limit of fracture scaling (l_{min}) with an expression ($\sigma_{truncation}$) analogous to equation (8). For small fractures of ellipticity λ:

$$\begin{aligned}\sigma_V &= \sum_{N=1}^{\infty}\frac{\pi l_N^2}{4\lambda} - \sum_{N=min}^{\infty}\frac{\pi l_N^2}{4\lambda} = \zeta\left(\frac{2}{e_V}\right)\frac{\pi l_1^2}{4\lambda} - \sigma_{truncation} \\ &= \frac{\pi}{4\lambda}l_1^2\left[1 + 2^{(-2/e_V)} + 3^{(-2/e_V)} + 4^{(-2/e_V)}\left(\frac{\frac{2}{e_V}+7}{2\left(\frac{2}{e_V}-1\right)}\right)\right] \\ &\quad - \frac{\pi}{4\lambda}l_{min}^2\frac{\frac{e_V}{2}}{1-\frac{e_V}{2}}\left[\left(\frac{l_1}{l_{min}}\right)^{e_V} + \frac{1}{2} + \frac{1}{2\frac{e_V}{2}}\right]\frac{l_{min+1}}{l_{min}} \\ &\cong \frac{\pi}{4\lambda}\left\{l_1^2\left[1 + 2^{(-2/e_V)} + 3^{(-2/e_V)} - 4^{(-2/e_V)}\left(\frac{2+7e_V}{2(e_V-2)}\right)\right]\right. \\ &\quad \left. + l_{min}^2\frac{e_V}{e_V-2}\left[\left(\frac{l_1}{l_{min}}\right)^{e_V} + \frac{1}{2} + \frac{1}{e_V}\right]\right\}.\end{aligned} \quad (10)$$

Consequently, for $e_V > 2$ or $e_S > 1$ the length of the smallest fractures in the population must be known in order to make a useful aggregate estimate of fracture surface area.

Most interpretations of fracture length scaling indeed suggest that $e_S > 1$ and $E_S > 1$ (e.g. see references under section entitled *Fracture scaling relations* above), so most fracture surface area should reside not in the largest fractures but in the smallest fractures. Data indicate that microfractures follow power-law scaling (Wong *et al.* 1989) that may be consistent with the scaling of larger fractures (McCaffrey *et al.* 1994). If this is the case, then, despite the relatively low values typical of specific fracture-surface energy (Scholz 1990, p. 114), the energy consumed during faulting by the generation of microfracture surface could be more significant than expected.

Extension fracture porosity

The aggregate fracture porosity of open extension fractures is analytically identical to the extensional strain produced by veins (i.e. filled extension fractures) (Gross & Engelder 1995), and equivalent to expressions for fault strain. The simplest form for expressing fracture porosity is based on one-dimensional sampling, because data or assumptions on fracture lengths are unneeded. For a one-dimensional sample of fracture apertures taken perpendicular to the orientation of fractures forming a perfectly aligned set, the aggregate fracture porosity (ϕ_T) of the fracture set is:

$$\phi_T = \sum \frac{b}{R_T} = \zeta\left(\frac{1}{c_T}\right)\frac{b_1}{R_T} = \zeta\left(\frac{1}{c_T}\right)a_T^{(1/c_T)}R_T^{(-1+(1/c_T))}. \quad (11)$$

As for fault strain, substitutions were made in deriving this result so as to specify fracture porosity in terms of the coefficient and exponent of the scaling law (neither of which will vary with sampling domain size) and the size of the sampling domain. Like fault strain, fracture porosity depends on sample size (except when the argument of the Riemann zeta function is equal to one) and generally is scale dependent. Equation (11) explicitly characterizes only one fracture set; multiple sets may be characterized by using equation (11) independently for each fracture set present in a rock mass and adding the results. If a distinction between large and small fractures is necessary, an expression equivalent to equation (9c) may be used. Values determined for c_T commonly fall between 0.7 and 0.9 (e.g. see references under section entitled *Fracture scaling relations* above), suggesting that the total fracture porosity for a population of open extension fractures is 2.9–9.6 times the porosity due to the single largest fracture. It is interesting that the scaling of extension fractures is so similar to the scaling of faults, perhaps implying that the same mechanism organizes the two types of fractures.

Extension fracture permeability

The aggregate fracture permeability of open extension fractures is most simply expressed using the 'cubic law' based on the parallel-plate model (e.g. Lamb 1932, Snow 1969). This model assumes single-phase laminar flow in fractures having smooth surfaces and constant aperture. The parallel-plate model additionally assumes that fractures are effectively infinite in length, so a one-dimensional sample of fracture apertures taken perpendicular to the orientation of a fracture set is sufficient to characterize permeability. Nelson (1985) discussed the treatment of multiple fracture sets, which requires the use of permeability tensors. Traditional application of the parallel-plate model uses average fracture aperture and spacing to characterize the scalar permeability parallel to a fracture set (e.g. Nelson 1985); however, this is a poor approach considering the power-law scaling of fractures. A better approach is to apply the parallel-plate model to each sampled fracture from a fracture set and sum the results. Thus, the aggregate fracture permeability (k_T) is:

$$k_T = \sum \frac{b^3}{12R_T} = \zeta\left(\frac{3}{c_T}\right)\frac{b_1^3}{12R_T}$$

$$= \frac{1}{12}\zeta\left(\frac{3}{c_T}\right)a_T^{(3/c_T)}R_T^{(-1+(3/c_T))}. \quad (12)$$

As for fault strain, substitutions were made in deriving this result so as to specify fracture permeability in terms of the coefficient and exponent of the scaling law (neither of which will vary with sampling domain size) and the size of the sampling domain. Again, fracture permeability depends on sample size (except when the argument of the Riemann zeta function is equal to one) and generally is scale dependent. If a distinction between large and small fractures is necessary, an expression similar to equation (9c) may be used. Values determined for c_T commonly fall between 0.7 and 0.9 (e.g. see references under *Fracture scaling relations* above), suggesting that the total fracture permeability for a population of open extension fractures is 1.06–1.15 times the permeability due to the single largest fracture. Even if the expression for fracture porosity is barely convergent [i.e. $c_T \approx 1$ in equation (11)], the total fracture permeability is only 1.20 times the permeability of the largest fracture. Thus, the single largest fracture in a sample should account for virtually all fracture permeability, but smaller fractures should account for most of the fracture porosity.

Extension fracture shear-wave anisotropy

Fluid-filled extension fractures significantly affect the transmission of seismic shear waves through rock (Crampin 1987, Thomsen 1995). Shear waves propagating in a direction parallel to the orientation of a set of fractures are split into components having particle motions parallel (velocity = v_{fast}) and transverse (veloc-

ity = v_{slow}) to the fractures and the resulting shear-wave anisotropy γ is defined by $v_{fast} = (1 + \gamma)v_{slow}$ (Thomsen 1995). The shear-wave anisotropy is fundamentally volumetric (the subscript is omitted here to avoid confusion with velocity) and may be written in terms of the fracture lengths (Thomsen 1995). Using the power-law scaling of the fracture lengths:

$$\gamma = \frac{1-v}{3(2-v)} \sum \frac{l^3}{R_V} = \frac{1-v}{3(2-v)} \zeta\left(\frac{3}{e_V}\right) \frac{l_1^3}{R_V}$$

$$= \frac{1-v}{3(2-v)} \zeta\left(\frac{3}{e_V}\right) h_V^{(3/e_V)} R_V^{(-1+(3/e_V))}, \qquad (13)$$

where v is Poisson's ratio. Substitutions were again made in deriving this result so as to specify shear-wave anisotropy in terms of the coefficient and exponent of the scaling law (neither of which will vary with sampling domain size) and the size of the sampling domain. Shear-wave anisotropy depends on sample size (except when the argument of the Riemann zeta function is equal to one) and generally is scale dependent. The scaling relations defined above may be used to express fracture porosity and permeability in terms of shear-wave anisotropy, providing a means of remotely quantifying the fluid-flow characteristics of a fracture population via seismic techniques.

DISCUSSION

A satisfactory understanding of scaling changes for fractures than span mechanically significant layers is yet to be developed. The formalism is available for describing such changes and incorporating them into descriptions of aggregate properties. However, existing observations are insufficient to adequately characterize the systematics across the large/small transition.

It is interesting that all of the aggregate properties addressed here yield scale-dependent expressions, except when the argument of the Riemann zeta function is one. In general, it appears that larger sampling domains should provide larger estimates of an aggregate property, at least over the range of scales in which fracture populations follow consistent scaling relations. This phenomenon has been observed in the case of fracture permeability (Clauser 1992), but well-documented examples for other aggregate properties have yet to be presented. The scale dependence of aggregate properties seems inconsistent with the common statement, based on power-law scaling of individual fracture attributes, that fracture populations are scale invariant. The reason for the scale dependence is that (except for fracture surface area) larger fractures contribute more to aggregate properties than do smaller fractures (when the argument of the Riemann zeta function is greater than one) and larger sampling domains statistically encompass larger fractures than do smaller sampling domains. The resulting effect may be visualized as self-affine geometry (e.g. Jackson & Sanderson 1992).

To date, the scaling relations of fractures have found their most widespread application in problems of fault strain and fault growth. However, it is clear that the scaling relations of fractures are useful for a variety of problems involving aggregate properties of fracture populations. The aggregate properties addressed here presumably represent only a small subset of interesting properties.

Acknowledgements—The Geology Foundation of the University of Texas at Austin, the Tectonic Studies Group and Amoco Production Co. provided funds for attending the 'Fault Populations' meeting. I thank K. McCaffrey, D. Peacock, R. Westaway and S. Wojtal for numerous useful criticisms and suggestions, although they may disagree with some of the conclusions.

REFERENCES

Apostal, T. M. 1957. *Mathematical Analysis*. Addison-Wesley, Reading, MA, U.S.A.

Baecher, G. B. & Lanney, N. A. 1978. Trace length biases in joint surveys. *U.S. Symp. Rock Mech.* **19**, 56–65.

Barton, C. A. & Zoback, M. D. 1992. Self-similar distribution and properties of macroscopic fractures at depth in crystalline rock in the Cajon Pass scientific drill hole. *J. geophys. Res.* **97**, 5181–5200.

Barton, C. C. & Hsieh, P. A. 1989. Physical and hydrologic-flow properties of fractures. 28th International Geological Congress Field Trip Guidebook T385, *Am. Geophys. Un.*, Washington, D.C., U.S.A.

Carter, K. E. & Winter, C. L. 1995. Fractal nature and scaling of normal faults in the Española Basin, Rio Grande rift, New Mexico: implications for fault growth and brittle strain. *J. Struct. Geol.* **17**, 863–873.

Childs, C., Walsh, J. J. & Watterson, J. 1990. A method for estimation of the density of fault displacements below the limit of seismic resolution in reservoir formations. In: *North Sea Oil and Gas Reservoirs II* (edited by Buller, A. T. *et al.*). The Norwegian Institute of Technology, Graham and Trotman, London, 309–318.

Cladouhos, T. T. & Marrett, R. 1996. Are fault growth and linkage models consistent with power-law distributions of fault lengths? *J. Struct. Geol.* **18**, 281–293.

Clauser, C. 1992. Permeability of crystalline rock. *Eos.* **73**, 233, 237–238.

Cowie, P. A. & Scholz, C. H. 1992. Displacement-length scaling relationship for faults: data synthesis and discussion. *J. Struct. Geol.* **14**, 1149–1156.

Crampin, S. 1987. Geological and industrial implications of extensive-dilatancy anisotropy. *Nature* **328**, 491–496.

Dahlquist, G. & Björck, Å. 1974. *Numerical Methods*. Prentice-Hall, Englewood Cliffs, NJ.

Davy, P. 1993. On the frequency–length distribution of the San Andreas fault system. *J. geophys. Res.* **98**, 12141–12151.

Dawers, N. H., Anders, M. H. & Scholz, C. H. 1993. Growth of normal faults: displacement–length scaling. *Geology* **21**, 1107–1110.

Gillespie, P. A., Walsh, J. J. & Watterson, J. 1992. Limitations of dimension and displacement data from single faults and the consequences for data analysis and interpretation. *J. Struct. Geol.* **14**, 1157–1172.

Gross, M. R. & Engelder, T. 1995. Strain accommodated by brittle failure in adjacent units of the Monterey Formation, U.S.A.: scale effects and evidence for uniform displacement boundary conditions. *J. Struct. Geol.* **17**, 1303–1318.

Gudmundsson, A. 1987a. Geometry, formation and development of tectonic fractures on the Reykjanes Peninsula, southwest Iceland. *Tectonophysics* **139**, 295–308.

Gudmundsson, A. 1987b. Tectonics of the Thingvellir fissure swarm, SW Iceland. *J. Struct. Geol.* **9**, 61–69.

Hatton, C. G., Main, I. G. & Meredith, P. G. 1993. A comparison of seismic and structural measurements of scaling exponents during tensile subcritical crack growth. *J. Struct. Geol.* **15**, 1485–1495.

Hatton, C. G., Main, I. G. & Meredith, P. G. 1994. Non-universal

scaling of fracture length and opening displacement. *Nature* **367**, 160–162.
Heffer, K. J. & Bevan, T. G. 1990. Scaling relationships in natural fractures—data, theory and applications. In: *Proc. Second European Petrol. Conf.*, SPE Paper 20981, 367–376.
Jackson, P. & Sanderson, D. J. 1992. Scaling of fault displacements from the Badajoz–Córdoba shear zone, SW Spain. *Tectonophysics* **210**, 179–190.
Johnston, J. D. 1992. The fractal geometry of vein systems: the potential for ore reserve calculation. In: *The Irish Minerals Industry* 1980–1990 (edited by Bowden, A. A., Earls, G., O'Connor, P. G. and Pyne, J.). Assoc. Econ. Geol., Dublin, 105–117.
Johnston, J. D. 1994. Fractal geometries of filled fracture systems—scaling of mechanisms. In: *Fault Populations* (edited by Cowie, P. A., Main, I. G. and Knipe, R.). Tectonic Studies Group Special Meeting, Edinburgh, 64–66.
Kakimi, T. 1980. Magnitude–frequency relation for displacement of minor faults and its significance in crustal deformation. *Bull. geol. Surv. Japan* **31**, 467–487.
Lamb, H. 1932. *Hydrodynamics*. Dover Publications, NY.
Main, I. G. 1992. Earthquake scaling. *Nature* **357**, 27–28.
Marrett, R. 1994. Scaling of intraplate earthquake recurrence interval with fault length and implications for seismic hazard assessment. *Geophys. Res. Lett.* **21**, 2637–2640.
Marrett, R. & Allmendinger, R. W. 1990. Kinematic analysis of fault-slip data. *J. Struct. Geol.* **12**, 973–986.
Marrett, R. & Allmendinger, R. W. 1991. Estimates of strain due to brittle faulting: sampling of fault populations. *J. Struct. Geol.* **13**, 735–738.
Marrett, R. & Allmendinger, R. W. 1992. Amount of extension on "small" faults: an example from the Viking graben. *Geology* **20**, 47–50.
McCaffrey, K. J. W., Johnston, J. D. & Feely, M. 1993. Use of fractal statistics in the analysis of Mo–Cu mineralisation at Mace Head, County Galway. Irish J. Earth Sci. **12**, 139–148.
McCaffrey, K. J. W., Johnston, J. D. & Loriga, M. A. 1994. Variation of fractal dimension in vein systems. In: *Fault Populations* (edited by Cowie, P. A., Main, I. G. & Knipe, R.). Tectonic Studies Group Special Meeting, Edinburgh, 103–105.
Nelson, R. A. 1985. *Geologic Analysis of Naturally Fractured Reservoirs*. Gulf Publishing, Houston.
Pacheco, J. F., Scholz, C. H. & Sykes, L. R. 1992. Changes in frequency–size relationship from small to large earthquakes. *Nature* **355**, 71–73.
Patton, T. L., Moustafa, A. R., Nelson, R. A. & Abdine, S. A. 1994. Tectonic evolution and structural setting of the Suez rift. In: *Interior Rift Basins* (edited by Landon, S. M.). *Am. Ass. Petrol. Geol. Mem.* **59**, 9–55.
Peacock, D. C. P. & Sanderson, D. J. 1993. Estimating strain from fault slip using a line sample. *J. Struct. Geol.* **15**, 1513–1516.
Peacock, D. C. P. & Sanderson, D. J. 1994. Strain and scaling of faults in the chalk at Flamborough Head, U.K. *J. Struct. Geol.* **16**, 97–107.
Romanowicz, B. & Rundle, J. B. 1993. On scaling relations for large earthquakes. *Bull. seism. Soc. Am.* **83**, 1294–1297.
Sanderson, D. J., Roberts, S. & Gumiel, P. 1994. A fractal relationship between vein thickness and gold grade in drill core from La Codosera, Spain. *Econ. Geol.* **89**, 168–173.
Scholz, C. H. 1990. *The Mechanics of Earthquakes and Faulting*. Cambridge University Press, Cambridge, U.K.
Scholz, C. H. 1994. A reappraisal of large earthquake scaling. *Bull. seism. Soc. Am.* **84**, 215–218.
Scholz, C. H. & Cowie, P. A. 1990. Determination of total strain from faulting using slip measurements. *Nature* **346**, 837–839.
Scholz, C. H., Dawers, N. H., Yu, J.-J., Anders, M. H. & Cowie, P. A. 1993. Fault growth and fault scaling laws: preliminary results. *J. geophys. Res.* **98**, 21951–21961.
Shaw, H. R. & Gartner, A. E. 1986. On the graphical interpretation of paleoseismic data. *U.S. geol. surv. Open-File Rep.* **86–394**.
Snow, D. T. 1969. Anisotropic permeability of fractured media. *Water Resources Res.* **5**, 1273–1289.
Thomsen, L. 1995. Elastic anisotropy due to aligned cracks in porous rock. *Geophys. Prosp.* **43**, 805–829.
Vermilye, J. M. & Scholz, C. H. 1995. Relations between vein length and aperture. *J. Struct. Geol.* **17**, 423–434.
Villemin, T. & Sunwoo, C. 1987. Distribution logarithmique self-similaire des rejêts et longueurs de failles: exemple du Bassin Houiller Lorrain. *C. r. Acad. Sci. Paris* **305**, 1309–1312.
Walsh, J. J. & Watterson, J. 1988. Analysis of the relationship between displacements and dimensions of faults. *J. Struct. Geol.* **10**, 239–247.
Walsh, J. J. & Watterson, J. 1992. Populations of faults and fault displacements and their effects on estimates of fault-related extension. *J. Struct. Geol.* **14**, 701–712.
Walsh, J. J., Watterson, J. & Yielding, G. 1991. The importance of small-scale faulting in regional extension. *Nature* **351**, 391–393.
Westaway, R. 1994. Quantitative analysis of populations of small faults. *J. Struct. Geol.* **16**, 1259–1273.
Wojtal, S. F. 1994. Fault scaling laws and the temporal evolution of fault systems. *J. Struct. Geol.* **16**, 603–612.
Wong, T.-F., Fredrich, J. T. & Gwanmesia, G. D. 1989. Crack aperture statistics and pore space fractal geometry of Westerly Granite and Rutland Quartzite: implications for an elastic contact model of rock compressibility. *J. geophys. Res.* **94**, 10267–10278.